Spin relaxation via exchange with donor impurity-bound electrons

Lan Qing, Jing Li, Ian Appelbaum, and Hanan Dery

Spin relaxation via exchange with donor impurity-bound electrons

Lan Qing,[1,2] Jing Li,[2] Ian Appelbaum,[2,*] and Hanan Dery[1,3]

[1]*Department of Physics and Astronomy, University of Rochester, Rochester, NY, 14627*
[2]*Department of Physics, Center for Nanophysics and Advanced Materials, U. Maryland, College Park, MD 20742*
[3]*Department of Electrical and Computer Engineering, University of Rochester, Rochester, NY, 14627*

At low temperatures, electrons in semiconductors are bound to shallow donor impurity ions, neutralizing their charge in equilibrium. Inelastic scattering of other externally-injected conduction electrons accelerated by electric fields can excite transitions within the manifold of these localized states. Promotion of the bound electron into highly spin-orbit-mixed excited states drives a strong spin relaxation of the conduction electrons via exchange interactions, reminiscent of the Bir-Aronov-Pikus process where exchange occurs with valence band hole states. Through low-temperature experiments with silicon spin transport devices and complementary theory, we reveal the consequences of this previously unknown spin depolarization mechanism both below and above the impact ionization threshold.

Spin exchange is central to many physical mechanisms that drive interactions between internal degrees of freedom in otherwise decoupled systems. In condensed-matter physics, exchange arises in diverse examples such as the well-known Overhauser and Knight effects between electron and nuclear spins[1–4], Glauber or Kawasaki kinetics in Ising models of ferromagnetism[5], and in the many-body RKKY and Kondo effects[6,7]. Within atomic physics, it is essential in optical pumping of noble gas nuclei for subsequent spin resonance detection[8,9]. The generality of this phenomenon extends even to the realm of particle physics, as in pion-nucleon isospin-exchange scattering at the Δ-resonance[10,11]. Direct impact on computing technology may one day occur as well, if robust qubits can be constructed from the spin of electrons bound to shallow donor impurity potentials in group-IV elemental semiconductors[12]. Spin exchange can then play an especially important role as the physical basis for state initialization and entanglement[13–16].

In this Rapid Communication, we demonstrate experimentally and describe theoretically how inelastic scattering between conduction and impurity-bound electrons leads to strong depolarization of both spins via mutual spin exchange. As we show with low-temperature spin transport measurements in unintentionally-doped silicon devices, this mechanism far outweighs the otherwise-dominant Elliott-Yafet spin relaxation mechanism[17,18]. The latter is mediated by the weak spin-orbit mixing of Pauli states in the conduction band of non-degenerate silicon[19–23]. Incorporating the exchange in a master equation approach successfully reproduces the observed nonlinear dependence of the charge and spin currents on temperature and electric field. In addition, this work includes a detailed formalism of the spin-dependent transitions in impurity states that may elucidate the physics relevant to terahertz laser emission from shallow donors in silicon[24].

As schematically shown in Fig. 1(a), our experiments utilize a ferromagnetic thin-film cathode to perform tunnel-junction injection of *spin-polarized* hot electrons into unintentionally very low-doped n-type Si(100): $L = 225$ micron-thick float-zone grown wafer with room-temperature resistivity $\rho \approx 5$ kΩ·cm[25]. This resistivity is two orders of magnitude less than that of intrinsic silicon, indicating the presence of highly-soluble phosphorus donors in our device at a level of approximately $N_d = 10^{12}$ cm^{-3}[26].

Figure 1(b) shows that for temperatures down to ≈ 25 K, the measured injection current (I_{C1}) of spin-polarized electrons is determined essentially only by the tunnel junction emitter voltage V_E (when qV_E exceeds the otherwise-rectifying Schottky barrier height of ≈ 0.7 eV at the metal thin-film contact interface). Furthermore, using a spin detector based on ballistic hot electron transport through a ferromagnetic thin film[27,28], we can measure the relative difference in spin transport signal between parallel and antiparallel injector/detector magnetic configurations as shown by sample data in the inset to Fig. 1(c). The spin polarization P derived from it rises and saturates as a function of internal electric field (V_{C1}/L) for 25 K and higher temperatures, as shown in Fig. 1(c). This behavior is due to the increase in drift velocity v and reduction in transit time through the Si transport region[29], from which a temperature-dependent spin lifetime τ can be determined in conjunction with spin precession measurements via $P \propto \exp(-\frac{L}{v\tau})$[30,31].

However, for lower temperatures this conventional behavior changes. Our central experimental result and the primary focus of this Rapid Communication is shown in Fig. 1(c). We find a stark change in the detected spin polarization when the temperature drops below 25 K: the spin polarization initially *decreases* with increasing electric field and eventually recovers to larger values at strong fields. We will find that this intriguing non-monotonic dependence is a result of inelastic spin-exchange scattering between conduction and localized electrons in the bulk silicon.

At these reduced temperatures, charge transport data in Fig. 1(b) shows that the injected current is rapidly suppressed for internal electric field $\mathcal{E} \lesssim 800$ V/cm, despite a constant incident flux of ballistic hot electrons impinging on the injection interface from a steady emitter voltage V_E. This transition temperature roughly corresponds to thermalization of conduction electrons into
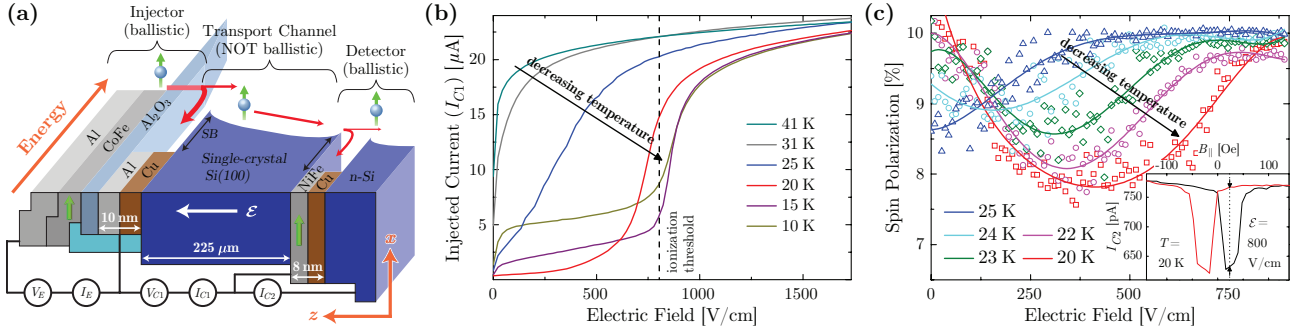
FIG. 1. (a) Schematic side view of the spin transport device. Energy band diagram is shown as depth into the page. Temperature dependence of (b) injected electron current, and (c) spin polarization from transport through a 225 μm-thick unintentionally doped Si device with approximately 10^{12} cm^{-3} donor concentration (the lines merely guide the eye). The hot electron injector tunnel junction voltage used here is $V_E = -1.3$ V, resulting in approximately 30 mA tunnel current that is unaffected by temperature or electric field in the Si transport region. The inset to (c) shows a characteristic spin-valve measurement from which the spin polarization can be determined (the magnetic field $B_\parallel$ is directed in the plane of the magnetic films).

the $E_{D^0} \approx 45$ meV donor state to form the D^0 neutral ground state below $\approx E_{D^0}/(k_B \ln N_c/N_d) \approx 30$ K, where N_c is the conduction band effective density of states. With the restoration of charge transport for $\mathcal{E} \gtrsim 800$ V/cm, the conduction electron spin polarization also recovers. Due to reduction in signal current from freeze-out effects in the detector portion of our device, spin polarization after transport can be measured only down to ≈ 20 K (i.e. $I_{C2} \to 0$ for $T < 20$ K).

To probe the electron transport in greater detail, spin precession measurements performed in an out-of-plane magnetic field can be used to determine the time-of-flight of electrons traveling through the Si channel with a transform method[31]. Results from these measurements are shown in Fig. 2. As temperature decreases from 30 K, mean transit times also initially decrease; this reduction is consistent with the expected higher mobility due to suppression in electron-phonon scattering. However, for temperatures below ≈ 25 K, transit times begin to *increase* in the same electric field region $\mathcal{E} \lesssim 800$ V/cm
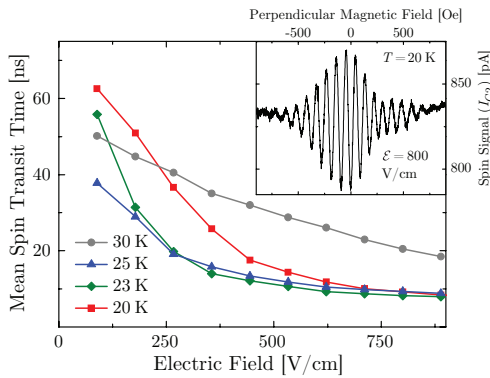

FIG. 2. Spin transit time through nominally undoped Si. Inset shows characteristic spin precession oscillations from which transit times are determined via Fourier transform at $\mathcal{E} = 800$ V/cm and $T = 20$ K.

where the charge current is suppressed. This behavior implies the role of transient interactions with impurity potentials in the electron transport[32].

Our physical picture used to explain this observed phenomena relies on inelastic scattering of energetic conduction band electrons with those bound to localized impurity potentials. "Impact excitation" occurs when the scattering event results in an excited but still bound state, and "impact ionization" when the donor-bound electron is liberated into the continuum of the conduction band[33]. The ionization rate is a strong function of the accelerating electric field; once it is comparable to the recombination rate (at the so-called "breakdown field"[34]) the free carrier concentration rises abruptly due to a chain reaction, similar to the multiplication process in "avalanche" photodetectors. As a result, nearly all donors are ionized above the breakdown field at any temperature.

The existence of impurity levels more weakly bound than the ground state can reduce this breakdown field ionization threshold. For example, once the localized electron is excited to the $2p_0$ state, it is more likely to undergo thermal activation to the conduction band[24]. The resulting < 1 kV/cm scale – lower than the regime needed to ignite significant intervalley f-process phonon scattering[35] – agrees well with the observed ionization threshold in Fig. 1(b).

Donor states in silicon are formed from the sixfold valley degeneracy of the conduction band; the $1s$ hydrogenic states are split by the crystal field ('valley-orbit interaction') into a nondegenerate $1s(A_1)$ ground state, a twofold-degenerate $1s(E)$ level, and a threefold-degenerate $1s(T_2)$ level[36]. Because of spin-orbit interaction, the latter state in particular becomes highly spin mixed $\Gamma_4 \to \Gamma_8 \oplus \Gamma_7$[36–38], in a way analogous to the p-like light and split-off hole states in the valence band of cubic semiconductors. Therefore, impact excitation from A_1 to T_2, accompanied by ~ 10 meV energy loss from the conduction electron[38], creates a superposition of station-
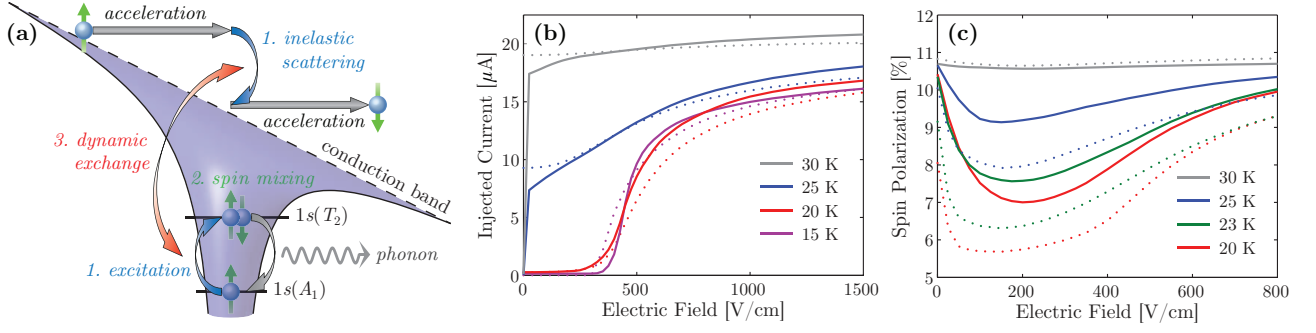
FIG. 3. (a) Simplified schematic of exchange-driven spin relaxation with neutral donors. In the first step, inelastic scattering with an accelerated conduction electron excites the bound electron ($A_1 \to T_2$). In the second step, ultrafast spin relaxation of the bound electron is facilitated by spin-mixing of the excited state (T_2). In the third step, the conduction-electron spin suffers relaxation via exchange. The electric field is exaggerated for illustrative purposes. Calculated (b) current and (c) spin polarization from transport through the silicon channel as a function of electric field. Solid lines are obtained from solution of the master equations [Eq. (3)], and dotted lines from the simplified model [Eqs. (1)-(2)]. These results reproduce the nonlinear dependencies on temperature and electric fields as measured in the experiment [Figs. 1(b)-(c)].

ary bound states whose spin precesses during time evolution. Upon subsequent stochastic phonon emission and return to the A_1 level, this spin is efficiently depolarized with respect to its initial orientation. As illustrated in Fig. 3(a), simultaneous exchange couples the conduction electron to this spin loss mechanism[39]. Similarly, spin depolarization of conduction electrons can be mediated via exchange between the unpolarized bound electron after its return to the A_1 state and a newly injected polarized electron that arrives at the impurity vicinity at later times[40,41], similar to conduction electron spin exchange with valence band holes in the well-known Bir-Aronov-Pikus relaxation mechanism[42].

We can thus qualitatively understand the trends in Fig. 1(c): Increasing electric field drives impact excitation and its concomitant conduction electron depolarization. This process continues until impact ionization at and above the breakdown field eliminates the population of bound electrons necessary for the process to occur. Spin polarization therefore is restored.

In an initial numerical model incorporating this phenomenology, we consider only a single effective impurity state i (i.e., ignoring their fine-structure, valley-orbit splitting, and different discrete levels) with depolarization caused by round-trip transitions to a spin-mixed state i'. Our spin injector sources spin density at a rate $P_J n_c R$, where P_J is initial spin polarization at injection (11.5% to match the experiment), n_c is the conduction electron number density, and R is the injection rate. The latter can be empirically estimated from injection current density ($\approx 10^{-1}$ A/cm^2) and the transport length as $\approx 10^8$ s^{-1}.

Spin relaxation due to the exchange-driven mechanism described here results in a measured conduction electron spin polarization P_c that is necessarily less than the injection polarization P_J. Conservation of angular momentum requires that the conduction electron spin density lost to the bound electrons per unit time [$n_c R (P_J - P_c)$]

is equal to the quantity gained by the impurity electron via elastic exchange [$\chi n_c n_i (P_c - P_i)$], where χ is the elastic exchange rate coefficient, and $n_i (P_i)$ is the impurity-bound electron density(spin polarization). In steady state, this same quantity is lost by the impurity to the environment [$P_i(\omega_{i,i'} n_i + \gamma_{i,i'} n_c n_i)$], where the first and last terms account for electron-phonon Castner-Orbach spin depolarization[38] with virtual transitions to a spin-mixed state i' (proportional to temperature-dependent rate coefficient $\omega_{i,i'}$) and inelastic exchange via impact excitation (proportional to the strongly electric-field-dependent coefficient $\gamma_{i,i'}$), respectively. Thus, we have the system of coupled equations

$$n_c R(P_J - P_c) = \chi n_c n_i (P_c - P_i)$$
$$= P_i(\omega_{\uparrow\downarrow} n_i + \gamma_{i,i'} n_c n_i). \qquad (1)$$

Along with the steady-state rate equation for conduction electron density

$$\omega_{i,c} n_i - \omega_{c,i} n_c + \gamma_{i,c} n_c n_i = \frac{dn_c}{dt} = 0, \qquad (2)$$

and local charge neutrality $n_i = N_d - n_c$, we can algebraically solve for both the conduction electron density which determines the measured current and the conduction electron polarization sensed by our spin detector. Here, $\omega_{i,c}$ is the phonon-assisted thermal (Arrhenius) transition rate into the conduction band, $\omega_{c,i}$ is the static thermalization rate, and $\gamma_{i,c}$ is the electric field-dependent impact ionization rate. Note that when the latter vanishes in zero-field equilibrium, this equation yields thermodynamic detailed balance.

The numerical results using appropriate coefficients obtained by comparison to experiment [e.g. Ref. 38] and Monte-Carlo simulations [e.g. Ref. 35], which should be compared to the corresponding experimentally measured values in Fig. 1(b)-(c), are shown by dotted lines

in Fig. 2(b)-(c). Even with this inexact, minimal model, they already reconcile the main trends in the empirical observations.

To remove the phenomenological nature of the simplified approach above, we can incorporate all the relevant processes with a system of general master rate equations for the occupations of the ℓth valley-orbit level with spin σ

$$
\frac{\partial n_{\ell\sigma}}{\partial t} = G_{\ell\sigma} + \overbrace{\sum_{\ell',\sigma'} (\omega_{\ell'\sigma',\ell\sigma} n_{\ell'\sigma'} - \omega_{\ell\sigma,\ell'\sigma'} n_{\ell\sigma})}^{\text{phonon absorption/emission}} \quad (3)
$$

$$
+ \overbrace{\sum_{\ell'\neq\ell,\sigma'\neq\sigma} \chi_{\ell,\ell'} (n_{\ell\sigma'} n_{\ell'\sigma} - n_{\ell\sigma} n_{\ell'\sigma'})}^{\text{elastic exchange}}
$$

$$
+ \underbrace{\sum_{\ell',\sigma',\sigma''} \left(\gamma^{\sigma''}_{\ell'\sigma',\ell\sigma} n_{\ell'\sigma'} n_{c\sigma''} - \gamma^{\sigma''}_{\ell\sigma,\ell'\sigma'} n_{\ell\sigma} n_{c\sigma''} \right)}_{\text{inelastic exchange + impact}},
$$

where we mark the separate terms with their physical meanings. Conduction electrons are denoted by $\ell = c$, and localized electrons by $\ell = 0, 1, 2 \ldots$ including all possible $1s$, $2s$, and $2p_0$ states with each comprised of twelve components (2 for spin and 6 for valley). $G_{\ell\sigma}$ denotes the conduction electron spin density lost to the bound electrons per unit time. As in the simple phenomenological model, the ω coefficients are phonon-assisted thermal transition rates, χ coefficients are the exchange rates (per unit density), and γ parameters are the electric field-dependent impact ionization or excitation rates (per unit density). Subscripts stand for the corresponding initial and final states, and superscripts of γ indicate the spins of impact conduction electrons, which accounts for the different nature of singlet and triplet scattering[43]. In this rigorous approach, all these rates are calculated directly from Fermi's golden rule to first order, except orbital-conserving spin-flip transitions necessarily involving two-phonon processes with virtual states, which are treated in second order[38]. The detailed calculations are given in the supplemental material[44], where we use Monte Carlo simulation to generate the energy distribution of electric field-heated conduction electrons[35,45], and include spatial dependence of $n_{\ell\sigma}$ by an exponential relation from the simple drift-diffusion model. We perform explicit time-domain simulation starting from fully ionized initial conditions to obtain the steady-state solution without any assumption of absolute charge neutrality. The results of this exact calculation for different electric field and temperature are summarized by the solid lines in Fig. 3(b)-(c) and agree with the experimental results shown in in Fig. 1(b)-(c).

The exchange spin relaxation mechanism shown by our experiment [Fig. 1(c)] and theory [Fig. 3(c)] outweighs the electron-phonon contribution[19] at low temperatures. Furthermore, it exists even without the accel-

erating electric field, in thermal equilibrium when it occurs due to energy loss by conduction electrons initially in the Maxwellian tail. As measured by Lépine, at low temperatures most of the donors are occupied by electrons and the conduction electron spin lifetime exhibits an anomalous increase with temperature[46]. The spin relaxation mechanism described here can easily account for this behavior: upon increase in temperature, the drop in neutral donor density outweighs enhancement of donor spin relaxation from higher thermal energy. The conduction electron spin flip rate associated with this exchange mechanism then falls with temperature until it competes with electron-phonon Elliott-Yafet spin relaxation to determine the total spin lifetime.

We have performed complementary experiments that exclude possible contributions to the observed phenomena from interface effects at the metal-semiconductor junction[47] as well as from electron-electron scattering in the conduction band[48]. As shown in Sec. 1 of the supplemental material, the exchange spin relaxation mechanism is not observed when we use shorter undoped silicon channels (10 μm), showing that interface effects are irrelevant. Furthermore, this effect is not due to the presence of the two-electron charged donor D^{-}[49], because these weakly-bound states form only at much lower temperatures[50]. The effect is most clearly observed when the densities of conduction and localized electrons are comparable, and when the channel is long enough such that injected electrons cannot avoid interacting with impurities on their way to the detector.

In closing, we notice that stimulated emission from the relevant $2p_0 \rightarrow 1s(E)$ transition in phosphorus doped silicon can be used for the realization of a terahertz laser[24]. The master equations presented in this Rapid Communication include both these states, so, along with spin-dependent radiative dipole selection rules, spin-polarized carrier injection may be shown to allow external control over circular polarization of the output terahertz electromagnetic field; in this case, alternative spin injection or generation schemes may be required such as interband optical orientation[51–54]. Meanwhile, since spin-polarized donor-bound electrons are integral to Kane's proposal for a phosphorus nuclear spin-based silicon quantum computing architecture[12], it is hoped that the picture unraveled in this work will yield insight relevant to the robustness of solid-state implementations of quantum information.

[*] appelbaum@physics.umd.edu

[1] A. W. Overhauser, Phys. Rev. **92**, 411 (1953).

[2] W. D. Knight, Phys. Rev. **76**, 1259 (1949).

[3] I. Solomon, Phys. Rev. **99**, 559 (1955).

[4] M. K. Chan, Q. O. Hu, J. Zhang, T. Kondo, C. J. Palmstrøm, and P. A. Crowell, Phys. Rev. B **80**, 161206 (2009).

[5] P. C. Hohenberg and B. I. Halperin, Rev. Mod. Phys. **49**, 435 (1977).

[6] A. Bayat, S. Bose, P. Sodano, and H. Johannesson, Phys. Rev. Lett. **109**, 066403 (2012).

[7] J. Kondo, J. Phys. Soc. Japan **1**, 1 (2005).

[8] T. G. Walker and W. Happer, Rev. Mod. Phys. **69**, 629 (1997).

[9] W. Happer, Rev. Mod. Phys. **44**, 169 (1972).

[10] S. J. Lindenbaum, Ann. Rev. Nuc. Sci. **7**, 317 (1957).

[11] M. Gell-Mann, Phys. Rev. **125**, 1067 (1962).

[12] B. Kane, Nature **393**, 133 (1998).

[13] D. Loss and D. P. DiVincenzo, Phys. Rev. A **57**, 120 (1998).

[14] J. R. Petta, A. C. Johnson, E. A. L. J. M. Taylor, A. Yacoby, M. D. Lukin, C. M. Marcus, M. P. Hanson, and A. C. Gossard, Science **309**, 2180 (2005).

[15] M. Anderlini, P. J. Lee, B. L. Brown, J. Sebby-Strabley, W. D. Phillips, and J. V. Porto, Nature **448**, 452 (2007).

[16] L. Amico, V. A. Doria, R. Fazio, and V. Vedral, Rev. Mod. Phys. **80**, 517 (2008).

[17] Y. Yafet, in *Solid State Physics*, Vol. 14, edited by F. Seitz and D. Turnbull (Academic Press, New York, 1963) pp. 1 – 98.

[18] R. Elliott, Phys. Rev. **96**, 266 (1954).

[19] P. Li and H. Dery, Phys. Rev. Lett. **107**, 107203 (2011).

[20] Y. Song and H. Dery, Phys. Rev. B **86**, 085201 (2012).

[21] J. L. Cheng, M. W. Wu, and J. Fabian, Phys. Rev. Lett. **104**, 016601 (2010).

[22] J.-M. Tang, B. T. Collins, and M. E. Flatté, Phys. Rev. B **85**, 045202 (2012).

[23] R. Jansen, Nature Mater. **11**, 400408 (2012).

[24] S. G. Pavlov, R. K. Zhukavin, E. E. Orlova, V. N. Shastin, A. Kirsanov, H.-W. Hübers, K. Auen, and H. Riemann, Phys. Rev. Lett. **84**, 5220 (2000).

[25] B. Huang, L. Zhao, D. J. Monsma, and I. Appelbaum, Appl. Phys. Lett. **91**, 052501 (2007).

[26] R. Thomas, H. Hobgood, P. Ravishankar, and T. Braggins, J. Crystal Growth **99**, 643 (1990).

[27] I. Appelbaum, B. Huang, and D. J. Monsma, Nature **447**, 295 (2007).

[28] Y. Lu and I. Appelbaum, Appl. Phys. Lett. **97**, 162501 (2010).

[29] M. Kameno, Y. Ando, E. Shikoh, T. Shinjo, T. Sasaki, T. Oikawa, Y. Suzuki, T. Suzuki, and M. Shiraishi, Appl. Phys. Lett. **101**, 122413 (2012).

[30] B. Huang, D. J. Monsma, and I. Appelbaum, Phys. Rev. Lett. **99**, 177209 (2007).

[31] B. Huang and I. Appelbaum, Phys. Rev. B **82**, 241202 (2010).

[32] Y. Lu, J. Li, and I. Appelbaum, Phys. Rev. Lett. **106**, 217202 (2011).

[33] V. V. Mitin, M. Asche, and H. Kostial, Phys. Rev. B **33**, 4100 (1986).

[34] W. Kaiser and G. H. Wheatley, Phys. Rev. Lett. **3**, 334 (1959).

[35] J. Li, L. Qing, H. Dery, and I. Appelbaum, Phys. Rev. Lett. **108**, 157201 (2012).

[36] W. Kohn, in *Solid State Physics*, Vol. 5, edited by F. Seitz and D. Turnbull (Academic Press, New York, 1957).

[37] Y. Song, O. Chalaev, and H. Dery, Phys. Rev. Lett. **113**, 167201 (2014).

[38] T. G. Castner, Phys. Rev. **155**, 816 (1967).

[39] Y. Ando, L. Qing, Y. Song, S. Yamada, K. Kasahara, K. Sawano, M. Miyao, H. Dery, and K. Hamaya, (2014), arXiv:1403.4509 [cond-mat].

[40] C. C. Lo, V. Lang, R. E. George, J. J. L. Morton, A. M. Tyryshkin, S. A. Lyon, J. Bokor, and T. Schenkel, Phys. Rev. Lett. **106**, 207601 (2011).

[41] R. N. Ghosh and R. H. Silsbee, Phys. Rev. B **46**, 12508 (1992).

[42] G. L. Bir, A. G. Aronov, and G. E. Pikus, Zh. Eksp. Teor. Fiz. **69**, 1382 (1975); Sov. Phys. JETP **42**, 705 (1975).

[43] A. Honig, Phys. Rev. Lett. **17**, 186 (1966).

[44] See Supplemental Material at http...for complementary experimental data on the effects of injected electron density and channel length, and for theory details on the impurity states, calculation of rate coefficients, solution of the master equations, and dynamic polarization of bound electrons. This material includes Refs. 24, 35, 36, 38, 43, 45, 46, 50, 55–64.

[45] C. Jacoboni and L. Reggiani, Rev. Mod. Phys. **55**, 645 (1983).

[46] D. J. Lépine, Phys. Rev. B **2**, 2429 (1970).

[47] Y. Lu, D. Lacour, G. Lengaigne, S. Le Gall, S. Suire, F. Montaigne, and M. Hehn, Appl. Phys. Lett. **103**, 022407 (2013).

[48] O. Dimitrova and V. Kravtsov, JETP Letters **86**, 749 (2008).

[49] Y. Lu, D. Lacour, G. Lengaigne, S. Le Gall, S. Suire, F. Montaigne, M. Hehn, and M. W. Wu, Appl. Phys. Lett. **104**, 042408 (2014).

[50] D. D. Thornton and A. Honig, Phys. Rev. Lett. **30**, 909 (1973).

[51] G. Lampel, Phys. Rev. Lett. **20**, 491 (1968).

[52] N. Sircar and D. Bougeard, Phys. Rev. B **89**, 041301 (2014).

[53] P. Li and H. Dery, Phys. Rev. Lett. **105**, 037204 (2010).

[54] P. Li, D. Trivedi, and H. Dery, Phys. Rev. B **87**, 115203 (2013).

[55] P. Giannozzi, S. de Gironcoli, P. Pavone, and S. Baroni, Phys. Rev. B **43**, 7231 (1991).

[56] V. V. Tsyplenkov, E. V. Demidov, K. A. Kovalevsky, and V. N. Shastin, Semicond. **42**, 1016 (2008).

[57] S. Rodriguez and T. Shultz, Phys. Rev. **178**, 1252 (1969).

[58] J. R. Chelikowsky and M. L. Cohen, Phys. Rev. B **14**, 556 (1976).

[59] M. J. Alguard, V. W. Hughes, M. S. Lubell, and P. F. Wainwright, Phys. Rev. Lett. **39**, 334 (1977).

[60] G. D. Mahan and R. Woodworth, Phys. Rev. B **78**, 075205 (2008).

[61] P. Y. Yu and M. Cardona, *Fundamentals of Semiconductors* (Springer, Berlin, 2010).

[62] G. D. Mahan, *Quantum Mechanics in a Nutshell* (Princeton University Press, Princeton, 2008).

[63] A. K. Ramdas and S. Rodriguez, Reports on Progress in Physics **44**, 1297 (1981).

[64] T. G. Castner, Phys. Rev. **130**, 58 (1963).